

# Supporting Information

Comparing Methods for Pyrite Surface Area Measurement Through Optical, Aqueous, and Gaseous Approaches

Samantha Macchi <sup>1</sup>, Martin Nemer <sup>2</sup>, Melissa M. Mills <sup>3</sup>, Melissa L. Meyerson <sup>4</sup>, Hans W. Papenguth <sup>1</sup>, John H. Taphouse <sup>5</sup> and Noah B. Schorr <sup>1,\*</sup>

<sup>1</sup> Power Sources R&D, Sandia National Laboratories, Albuquerque, NM 87185, USA

<sup>2</sup> Energy, Multi Phase, Soft Matter R&D, Sandia National Laboratories, Albuquerque, NM 87185, USA

<sup>3</sup> Nuclear Waste Disposal Research & Analysis, Sandia National Laboratories, Albuquerque, NM 87185, USA

<sup>4</sup> Materials Characterization & Performance, Sandia National Laboratories, Albuquerque, NM 87185, USA

<sup>5</sup> Battery Design & Development, Sandia National Laboratories, Albuquerque, NM 87185, USA

\* Correspondence: nschorr@sandia.gov

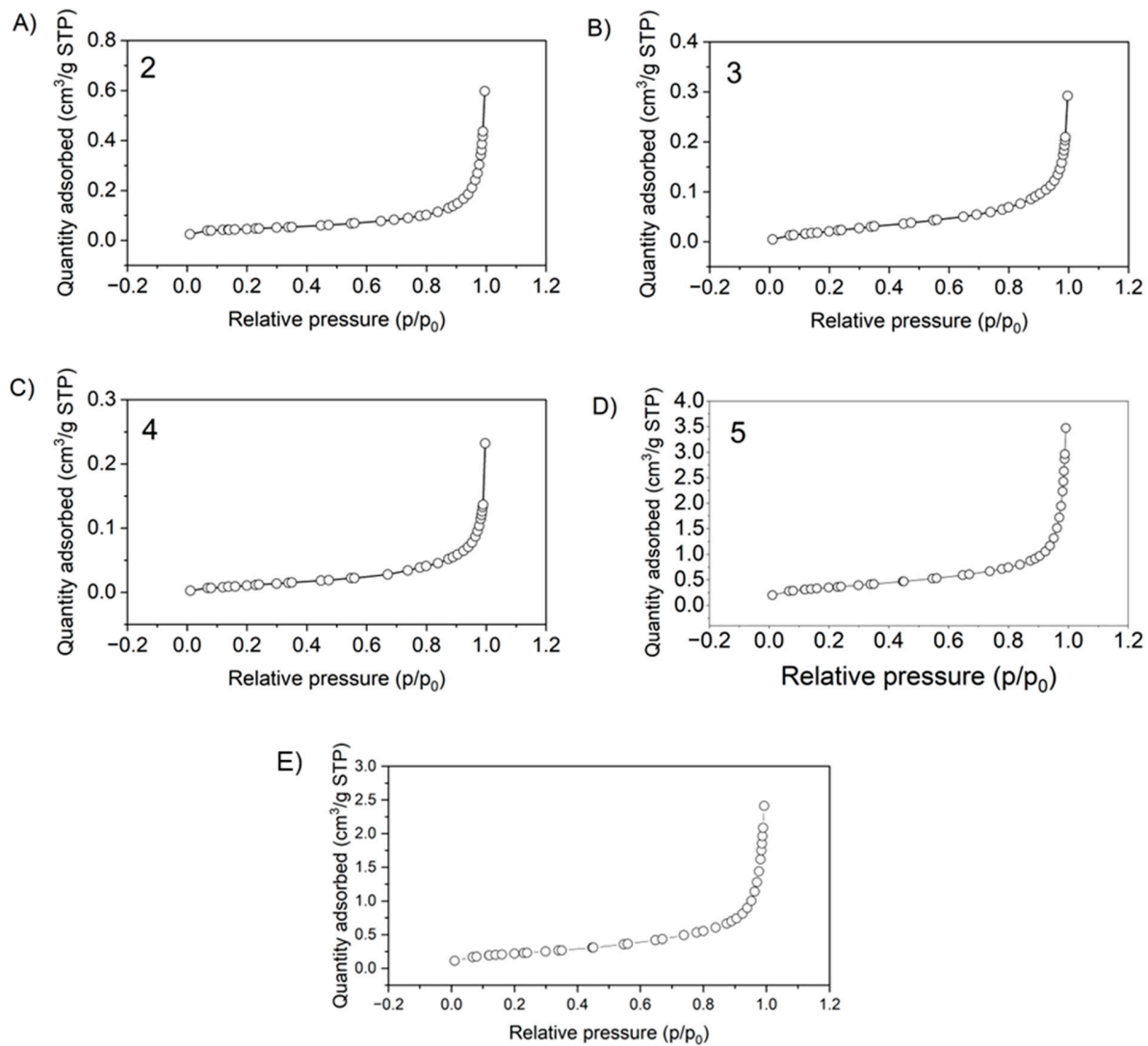


Figure S1. BET isotherm plots for sample 2-5 with 1 g sample mass.

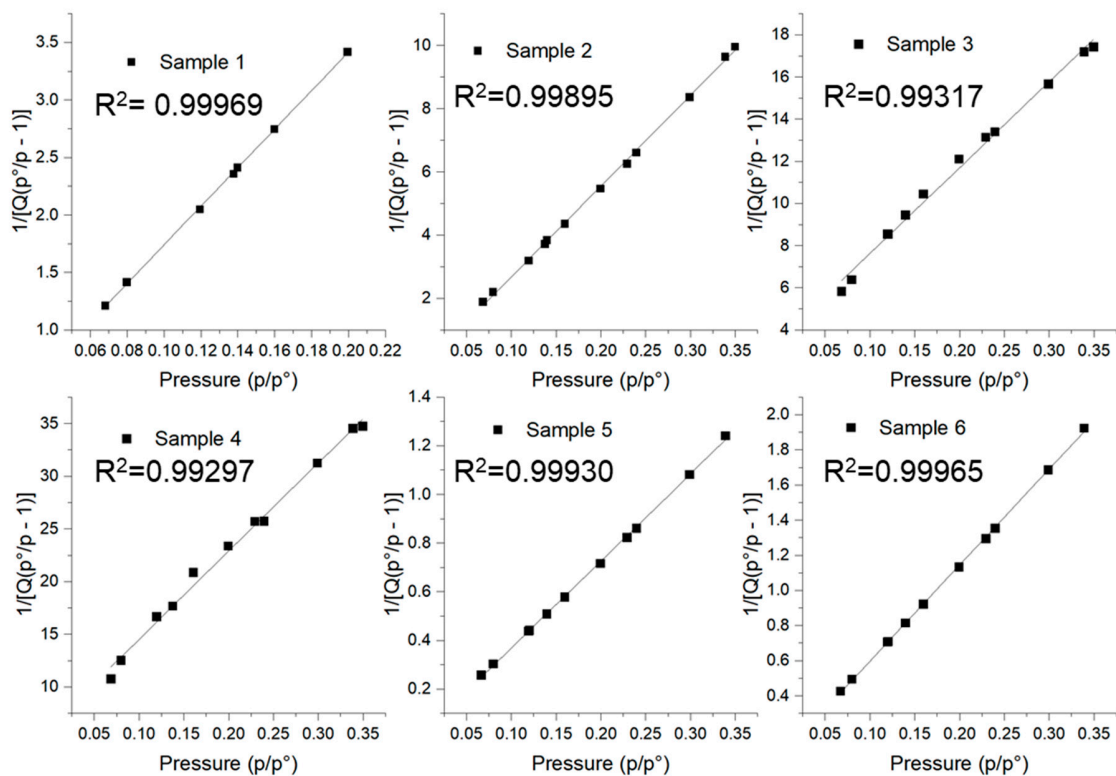


Figure S2. Nitrogen sorption BET isotherms of samples 1-6 with fitting results.

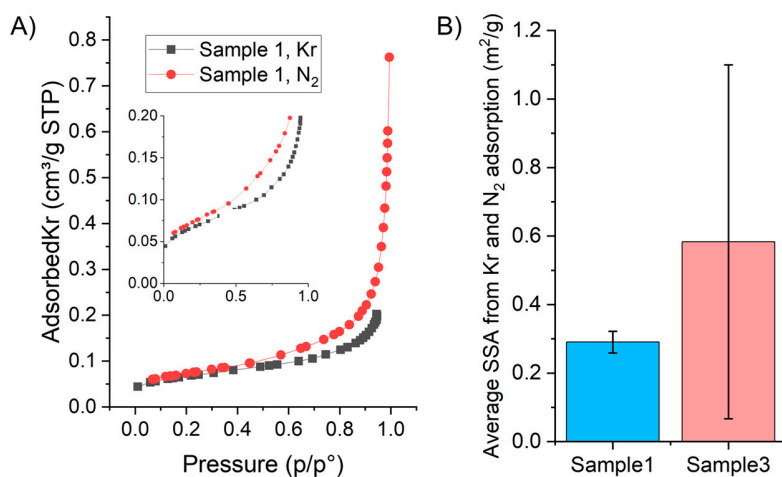


Figure S3. A) Adsorption isotherms of sample 1 with  $\text{N}_2$  and Kr gas and B) average SSA values from Kr and  $\text{N}_2$  adsorption for sample 1 and 3.

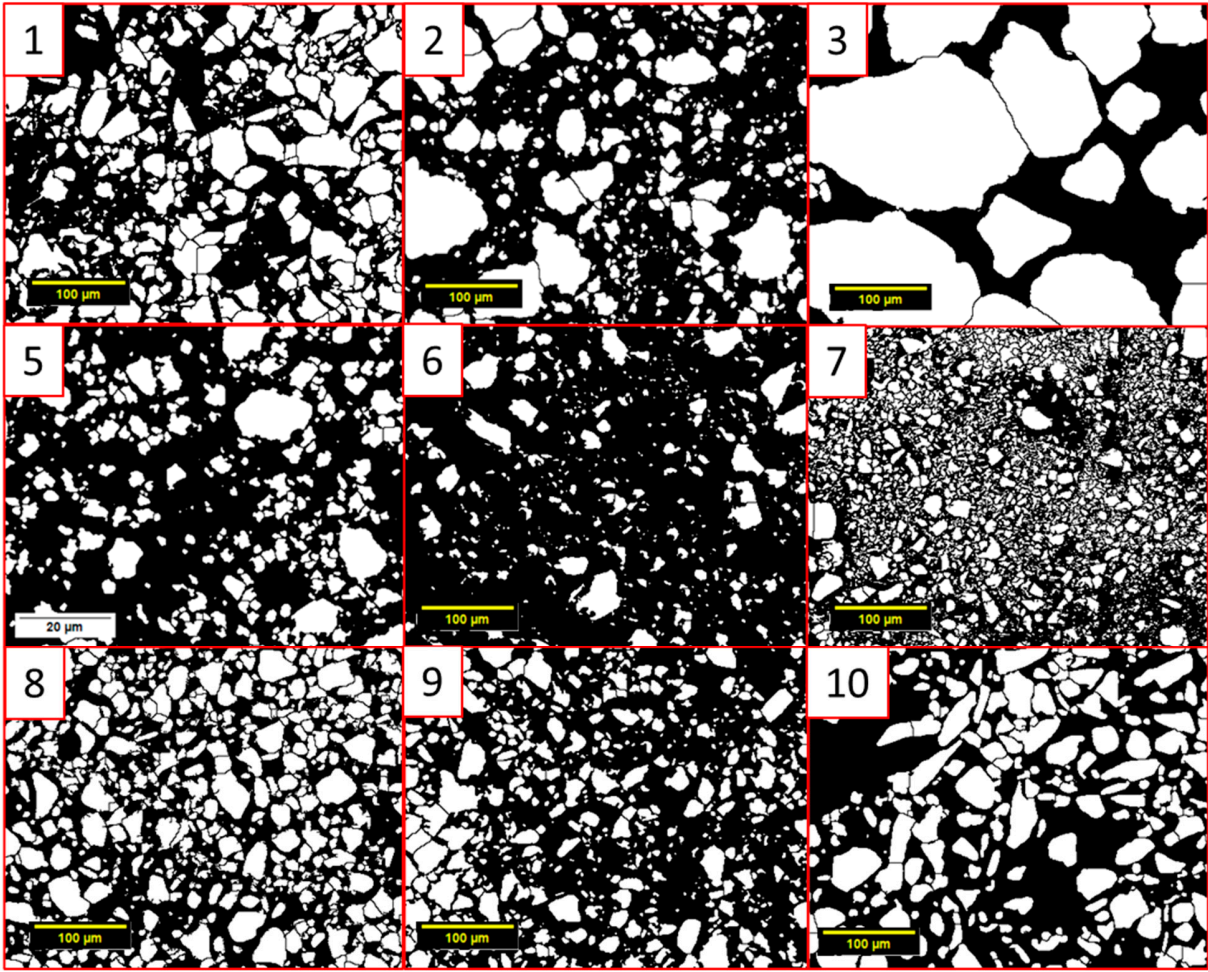


Figure S4. 2D projections from SEM micrograph images of sample 1-10, excluding sample 4 which is shown in main text.

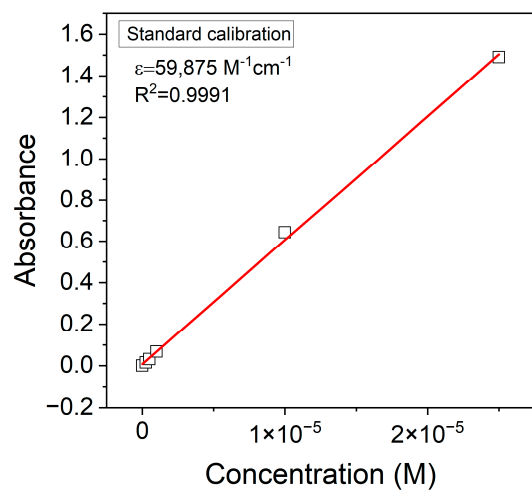


Figure S5. Calibration curve of MB in water.

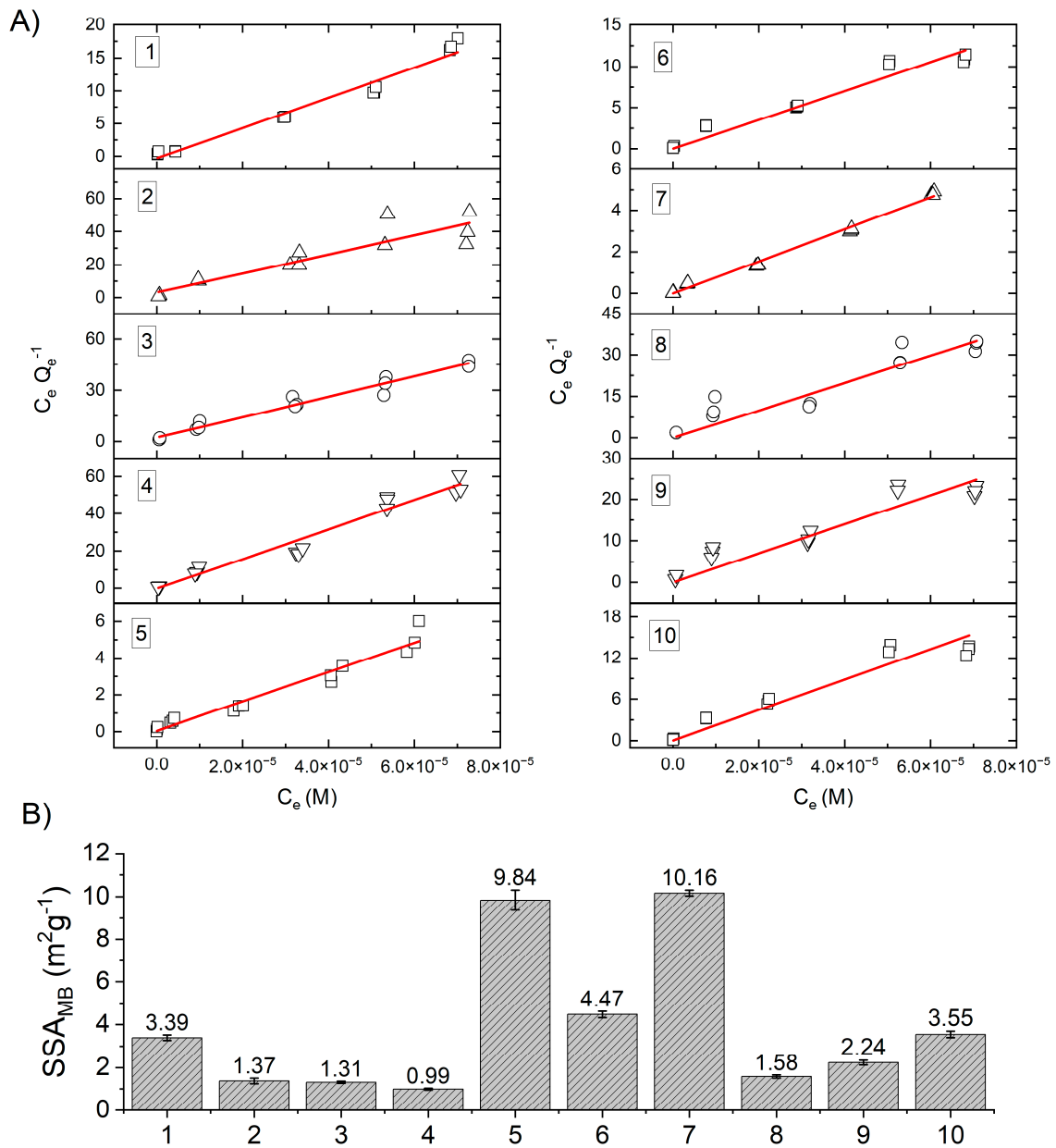


Figure S6. A) Plot of  $C_e Q_e^{-1}$  vs  $C_e$  for  $FeS_2$  samples 1-10 and B) resultant  $SSA_{MB}$  values.

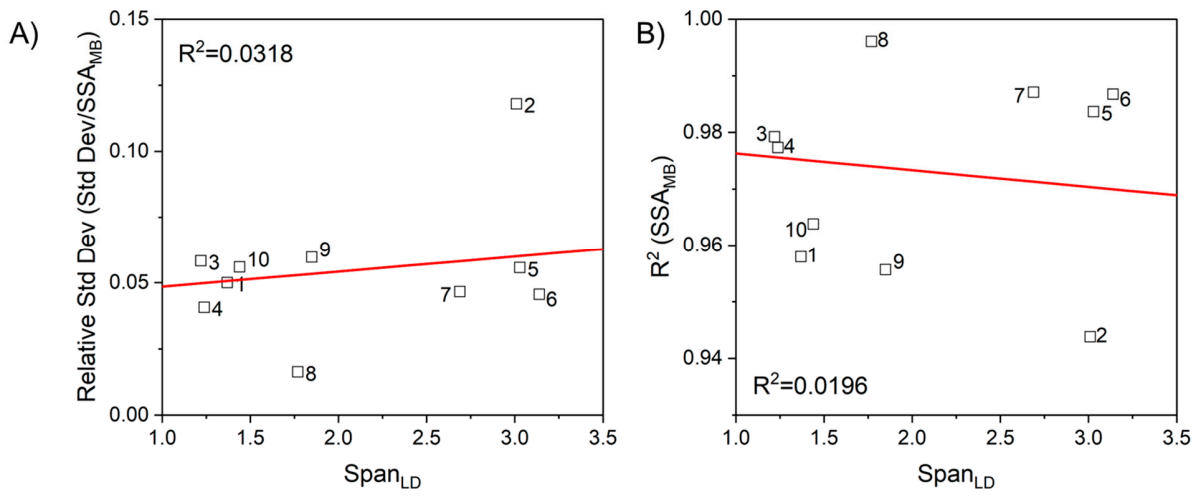


Figure S7. A) Dependence of relative standard deviation and B) dependence of goodness of fit ( $R^2$ ) of SSA<sub>MB</sub> on span<sub>LD</sub>.

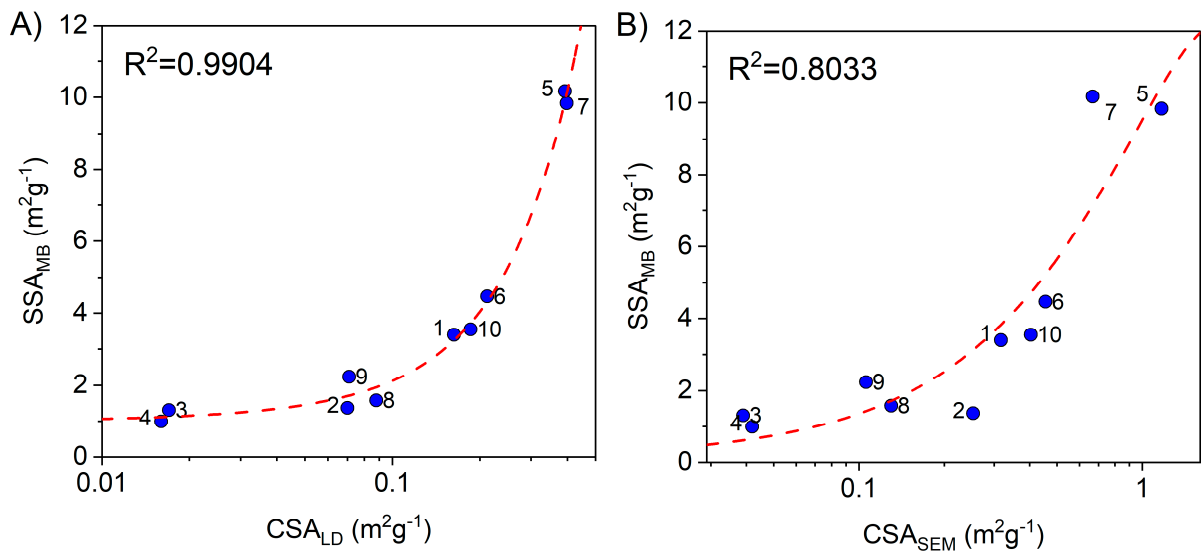


Figure S8. Parabolic fitting of A) CSA<sub>LD</sub> versus SSA<sub>MB</sub>, and B) CSA<sub>SEM</sub> versus SSA<sub>MB</sub>. The parabolic relationship between CSA<sub>LD</sub> and SSA<sub>MB</sub> is hypothesized to be due to biasing of larger particles by LD.

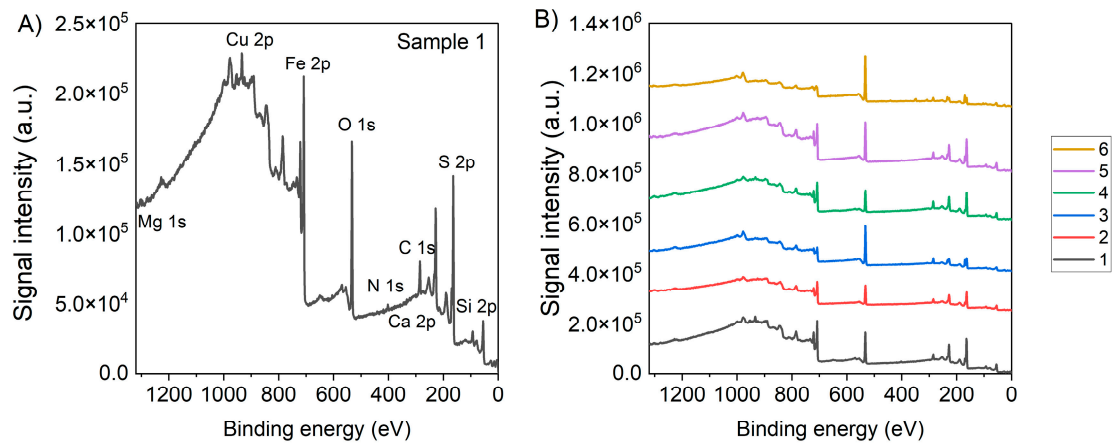


Figure S9. XPS A) Survey scan of sample 1 showing binding energy of elements of interest and B) survey scan of samples 1-6.

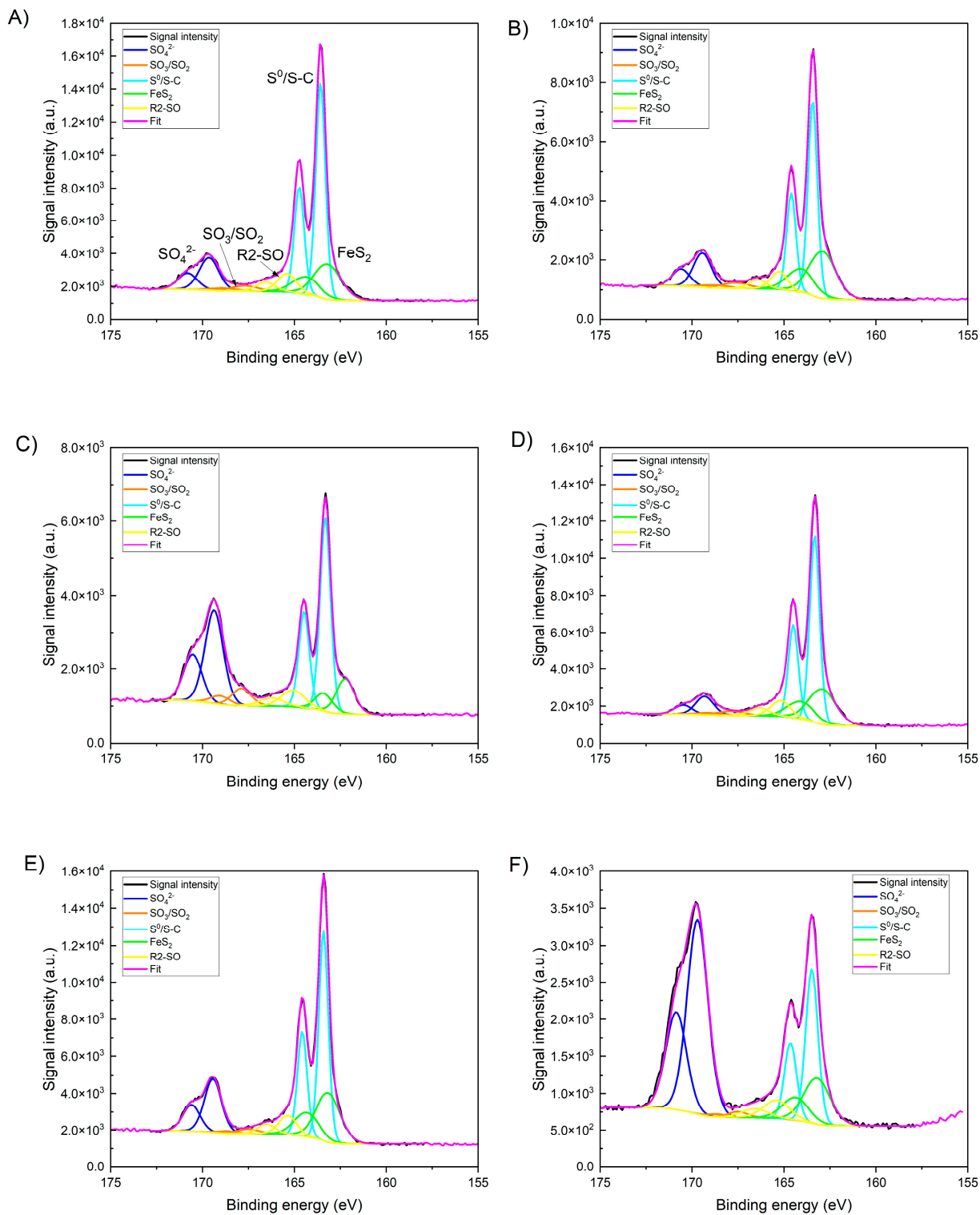


Figure S10. XPS narrow scans of sulfur of sample A) 1, B) 2, C) 3, D) 4, E) 5, F) 6.

Table S1. XPS survey scan atomic percentages of elements present in FeS<sub>2</sub> samples 1-6.

Sample	Fe 2p	S 2p	O 1s	C 1s	N 1s	Mg 1s	Si 2p	Ca 2p	Cu 2p
1	11.8	36.0	33.4	15.5	1.2	0.0	0.0	0.0	2.0
2	10.2	35.7	35.5	17.6	1.0	0.0	0.0	0.0	0.0
3	3.6	21.5	50.7	22.9	0.7	0.3	0.0	0.0	0.4
4	9.7	32.8	27.6	27.0	1.7	0.0	0.0	0.0	1.2
5	8.4	32.4	36.6	21.7	0.7	0.2	0.0	0.0	0.0
6	4.2	18.5	58.9	13.4	0.6	0.7	2.0	1.7	0.0

Table S2. XPS relative atomic percentages of surface sulfur-containing functional groups present in FeS<sub>2</sub> samples 1-6.

Sample	FeS <sub>2</sub>	R2-SO	S <sup>0</sup> /S-C	SO <sub>3</sub> <sup>2-</sup> /SO <sub>2</sub> -C	SO <sub>4</sub> <sup>2-</sup>
1	21.9	8.3	50.7	3.5	15.6
2	33.7	7.6	39.4	4.4	14.9
3	13.8	7.1	36.1	6.2	36.8
4	37.3	8.2	41.1	4.1	9.2
5	21.9	8.3	48.3	2.2	19.2
6	17.2	6.3	23.7	1.2	51.6

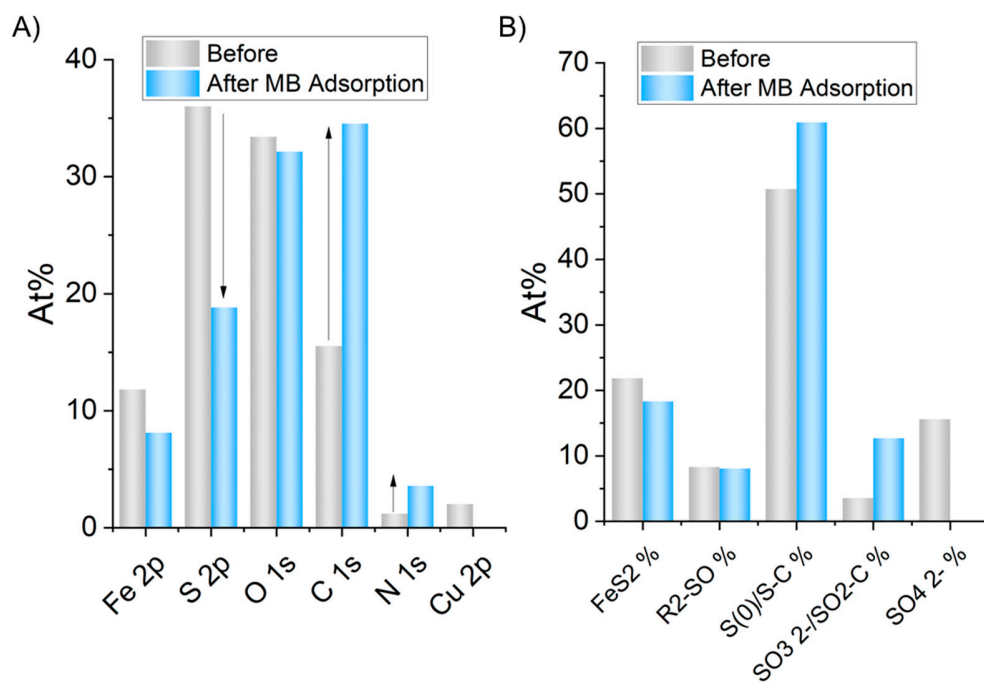


Figure S11. Atomic percentages from XPS A) survey scans and B) narrow scans of sulfur of sample 1 before and after MB adsorption. The sample was removed via centrifugation followed by 3x wash with DI water and dried under vacuum at 60 °C for 48 hr to remove moisture.